



# Physiologically Based Precision Dosing Approach for Drug-Drug-Gene Interactions: A Simvastatin Network Analysis

Jan-Georg Wojtyniak<sup>1,2</sup> , Dominik Selzer<sup>1</sup>, Matthias Schwab<sup>2,3,4</sup> and Thorsten Lehr<sup>1,\*</sup> 

Drug-drug interactions (DDIs) and drug-gene interactions (DGIs) are well known mediators for adverse drug reactions (ADRs), which are among the leading causes of death in many countries. Because physiologically based pharmacokinetic (PBPK) modeling has demonstrated to be a valuable tool to improve pharmacotherapy affected by DDIs or DGIs, it might also be useful for precision dosing in extensive interaction network scenarios. The presented work proposes a novel approach to extend the prediction capabilities of PBPK modeling to complex drug-drug-gene interaction (DDGI) scenarios. Here, a whole-body PBPK network of simvastatin was established, including three polymorphisms (*SLC01B1* (rs4149056), *ABCG2* (rs2231142), and *CYP3A5* (rs776746)) and four perpetrator drugs (clarithromycin, gemfibrozil, itraconazole, and rifampicin). Exhaustive network simulations were performed and ranked to optimize 10,368 DDGI scenarios based on an exposure marker cost function. The derived dose recommendations were translated in a digital decision support system, which is available at [simvastatin.precisiondosing.de](https://simvastatin.precisiondosing.de). Although the network covers only a fraction of possible simvastatin DDGIs, it provides guidance on how PBPK modeling could be used to individualize pharmacotherapy in the future. Furthermore, the network model is easily extendable to cover additional DDGIs. Overall, the presented work is a first step toward a vision on comprehensive precision dosing based on PBPK models in daily clinical practice, where it could drastically reduce the risk of ADRs.

## Study Highlights

### WHAT IS THE CURRENT KNOWLEDGE ON THE TOPIC?

✔ Drug-drug interactions (DDIs), drug-gene interactions, and drug-drug-gene interactions (DDGIs) are well known triggers of adverse drug reactions that might be preventable by precision dosing. One example compound prone to DDGIs is simvastatin.

### WHAT QUESTION DID THIS STUDY ADDRESS?

✔ How physiologically based pharmacokinetic (PBPK) modeling can be utilized for model-informed precision dosing (MIPD) of complex DDGIs.

### WHAT DOES THIS STUDY ADD TO OUR KNOWLEDGE?

✔ This study presents whole-body PBPK models for simvastatin lactone and simvastatin acid, including variation of four

pharmacogenes and was tested against four DDI perpetrator drugs and one DDI victim. In addition, the model was used to develop a digital decision support system based on dose recommendations for 10,368 simulated interaction scenarios.

### HOW MIGHT THIS CHANGE CLINICAL PHARMACOLOGY OR TRANSLATIONAL SCIENCE?

✔ The presented dose recommendations might help to better assess risks of simvastatin therapy in pharmacogenomic and polypharmacy context. Furthermore, the study highlights and guides how PBPK can help to bring MIPD into daily clinical practice.

Adverse drug reactions (ADRs) are a burden to our health care and economic systems. The US Food and Drug Administration (FDA) assumes that annually > 2,216,000 serious ADRs in hospitalized patients lead to over 106,000 deaths in the United

States—ranking them as the fourth leading cause of death.<sup>1,2</sup> The associated costs are tremendous and are estimated to add up to US \$200 billion per year.<sup>1</sup> This situation is likely to become more acute as a result of ever-growing prescription use. According to

<sup>1</sup>Clinical Pharmacy, Saarland University, Saarbrücken, Germany; <sup>2</sup>Dr. Margarete Fischer-Bosch-Institute of Clinical Pharmacology, Stuttgart, Germany; <sup>3</sup>Departments of Clinical Pharmacology and Pharmacy and Biochemistry, University of Tübingen, Tübingen, Germany; <sup>4</sup>Cluster of Excellence iFIT (EXC2180) "Image-guided and Functionally Instructed Tumor Therapies", University of Tübingen, Tübingen, Germany. \*Correspondence: Thorsten Lehr ([thorsten.lehr@mx.uni-saarland.de](mailto:thorsten.lehr@mx.uni-saarland.de))

Received August 4, 2020; accepted November 7, 2020. doi:10.1002/cpt.2111

the Centers for Disease Control and Prevention, the proportion of Americans taking > 5 prescription drugs on a regular basis has almost tripled in the past 20 years.<sup>3</sup>

Drug-drug interactions (DDIs) and drug-gene interactions (DGIs) are the most common reasons for ADRs.<sup>2,4,5</sup> Unfortunately, in current clinical practice DDIs and DGIs are considered separate entities that are typically handled in a nonholistic fashion.<sup>4</sup> However, as shown recently, 19% of potentially clinically significant interactions occur as a combination of DDIs and DGIs (drug-drug-gene interaction (DDGIs)).<sup>4,5</sup> Tackling DDIs, DGIs, or DDGIs using guidelines on dose adaptation could reduce the number of ADRs substantially, because it is assumed that 80% of ADRs

are dose-related and, hence, could be prevented.<sup>6,7</sup> This concept can be summarized as precision dosing for DDIs and DGIs.<sup>8</sup>

The current approach of developing such guidelines would be the investigation of DDGIs in clinical trials analogous to presently conducted trials on DDIs and DGIs.<sup>8,9</sup> Those studies are typically performed in healthy volunteers, in a homogenous study population and with a controlled treatment plan (**Figure 1a**).<sup>8</sup> Consequently, they do not reflect the situation in multimorbid patients, affected by polypharmacy and genetic polymorphisms, which is the patient group most susceptible to ADRs (**Figure 1b**).<sup>1,8</sup> Moreover, due to the combinatorial explosion of all possible DDGIs, exhaustive studies might not be feasible at all (**Figure 1c**).

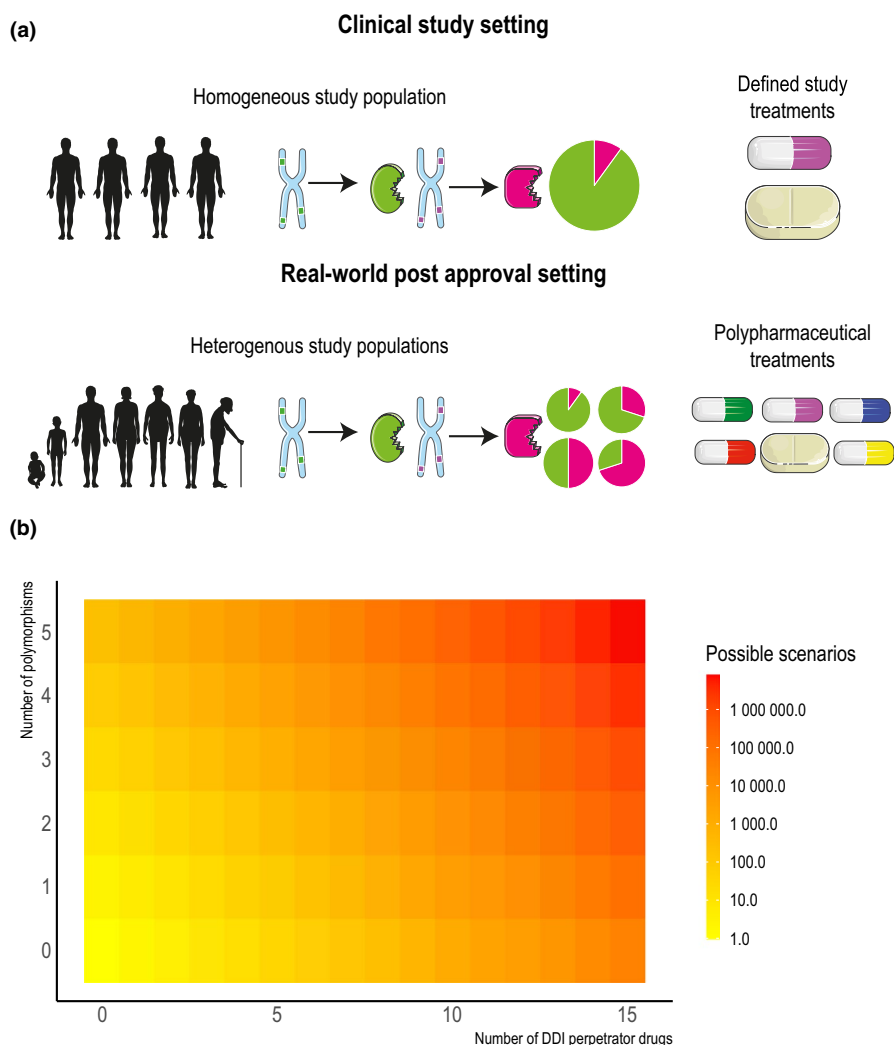


**Figure 1** Difference between a clinical study setting and a real-world post-approval setting. **(a)** The upper part shows the research situation in a clinical setting. A homogenous study population receives a defined treatment regimen in a standardized procedure. The subsequently obtained results are used for the development of therapy recommendations for the post-approval setting. The lower part depicts the real-world postapproval setting with a higher variability in demographics, variant distribution, and a higher degree in polypharmacy compared with the clinical study population. As a result, as shown in **(b)** various possible DDGI scenarios are conceivable depending on the amount of concomitantly used perpetrator drugs and occurring polymorphisms. For the calculation it was assumed that each perpetrator has two DDI states (perpetrator is given or perpetrator is not given) and each clinically relevant polymorphism could have three independent phenotypes. Following the number of possible scenarios was calculated with  $n_{\text{scenarios}} = 2^x_{\text{perpetrator}} * 3^y_{\text{polymorphism}}$ . The increase of possible DDGI scenarios is shown as a heatmap. The number of possible DDGI scenarios is shown on a log-scale. Some figure elements are taken from smart.servier.com (CC BY 3.0). DDGI, drug-drug-gene interaction; DDI, drug-drug interaction. [Colour figure can be viewed at wileyonlinelibrary.com]

To overcome this problem, a promising approach would be the application of whole-body physiologically based pharmacokinetic (PBPK) modeling.<sup>4</sup> PBPK models hold the capability to predict the DDGI potential of drugs *in silico* and to develop alternative precision dosing regimens for patients.<sup>4</sup> The reliability of this technique has already been demonstrated in several DDI and DGI studies and is acknowledged by regulatory agencies.<sup>10–12</sup> However, although PBPK modeling has been accepted as a useful option to predict the extent of DDGIs, examples on how PBPK modeling can be used for model informed precision dosing (MIPD) are still scarce.<sup>12</sup>

Thus, the aim of this work was to illustrate the complexity of DDIs, DGIs, and DDGIs based on the example of simvastatin. Simvastatin was selected as it is among the most prescribed drugs in industrial nations and is highly susceptible to potentially life-threatening ADRs due to its complex pharmacokinetics (PKs).<sup>13–18</sup> Moreover, this work should provide guidance for the development of an PBPK-based MIPD approach. Therefore, a comprehensive simvastatin DDGI PBPK network model was implemented to serve a web-based decision support system that offers quick and easy access to optimized dose recommendations for individual patients.

## METHODS

### Software

PBPK model development was performed with PK-Sim and MoBi (version 8 – Build 21) as part of the Open Systems Pharmacology Suite.<sup>19</sup> Model parameter identification was accomplished using Monte-Carlo optimization. Local sensitivity analysis was also performed within PK-Sim. Published plasma concentration-time profiles were digitized using GetData Graph Digitizer (version 2.26.0.20, S. Fedorov).<sup>20</sup> Graphics and statistical analysis were produced and implemented using R (version 3.6.3).<sup>21</sup>

### Simvastatin PBPK model building

The simvastatin model was developed in a stepwise procedure. In a first step, physicochemical parameters of simvastatin lactone (SL) and simvastatin acid (SA) as well as information on absorption, distribution, metabolism, and excretion processes were extracted from literature. Subsequently, mean plasma concentration-time profiles of SL and SA after oral single dose and multiple dose administration were digitized from published studies and separated into training and test datasets for model development and evaluation, respectively. Model input parameters, which were not available as PK-Sim reference values or that could not be informed from published literature values were optimized by fitting the model to measured plasma concentration-time profiles from the training dataset. PBPK study simulations were built based on healthy individuals with the reported mean values for age, weight, height, and genetic background, as stated in the corresponding study protocol, respectively. If parameter information was lacking, a PK-Sim mean individual (healthy male European, 30 years of age, body weight of 73 kg, a height of 176 cm, and based on the International Commission on Radiological Protection database) with wild type genotype was substituted. For all simulated individuals, glomerular filtration and enterohepatic cycling was implemented. A detailed description of the model development process, including information about digitized studies and model parameters can be found in the **Supplementary Material, chapter 2**.

### DGI implementation and DDI network development

DGI effects were implemented assuming a changed enzyme turnover number ( $k_{cat}$ ) compared with wild type. Here, the homozygous wild type  $k_{cat}$  as well as  $k_{cat}$  for homozygous polymorphic individuals were

estimated during model training (see **Supplementary Material, chapter 1.1.2** and **chapter 2.4**).

A DDI network was built to further evaluate the performance of the developed model. Thus, previously developed models of clarithromycin, gemfibrozil, itraconazole, rifampicin, and midazolam were coupled with the simvastatin model.<sup>12,22,23</sup> Population mean profiles as well as area under the curve (AUC) and peak plasma concentration ( $C_{max}$ ) values were predicted and compared against observed study data to evaluate the network quality.<sup>20</sup>

A detailed overview on the implementation of the DDI network, including relevant interaction parameters from *in vitro* experiments as well as the mathematical implementation of the drug interaction processes, is provided in the **Supplementary Material in chapter 1** and **chapter 3**.

### PBPK network evaluation and sensitivity analysis

PBPK model evaluation was performed using different statistical and graphical evaluation techniques. Predicted plasma concentration-time profiles were compared with observed profiles. Moreover, goodness-of-fit plots for predicted vs. observed plasma concentrations were examined. Mean relative deviation<sup>24</sup> and median symmetric accuracy<sup>25</sup> were calculated for all differences between observed and predicted plasma concentrations. In addition, the performance was evaluated by comparison of the noncompartmental analysis parameters AUC from last dose to last observation and  $C_{max}$ . AUC was computed using a linear-up log-down method. Geometric mean fold errors (GMFEs) were derived for differences between observed and predicted AUC and  $C_{max}$  values. For DGI and DDI predictions, AUC effect ratios were compared, in which a deviation of the observed from the predicted effect ratio less than two times was considered sufficient. Finally, local sensitivity analysis of the final model to single parameter changes was calculated as relative changes of the AUC of one dosing interval in steady-state conditions. A detailed overview of performance measurements and the local sensitivity analysis can be found in the **Supplementary Material, chapter 1.4**.

### Dose optimization

Simvastatin dose optimization for several DDGI scenarios, including individual DDIs and DGIs was performed. As reference, plasma concentration-time profiles for SL and SA in a mean individual after administration of 5 mg up to 80 mg (5 mg steps) SL once daily for 7 days were simulated and SL and SA AUCs from the time of the last dose up to 24 hours postdose derived. In a second step, a DDGI matrix was set up covering every possible combination of the three polymorphisms *SLCO1B1* (rs4149056), *ABCG2* (rs2231142), and *CYP3A5* (rs776746) and comedication with the four perpetrator drugs clarithromycin, itraconazole, gemfibrozil, and rifampicin. DDGI scenarios were simulated with administered SL doses according to the reference (7 days + 24 hours postdose) and reasonable perpetrator dosing regimens (see **Table 1**). For each simulation, SL and

**Table 1** Investigated perpetrator regimens

| Perpetrator    | Half-life, monotherapy | Regimen  |
|----------------|------------------------|--|
| Clarithromycin | 3.3–4.9 hours          | 500 mg b.i.d.                                  |
| Itraconazole   | ~ 24 hours             | 200 mg daily                                   |
| Rifampicin     | 2.5 hours              | 600 mg daily concomitant with simvastatin      |
| Rifampicin     | 2.5 hours              | 600 mg daily 17 hours after simvastatin dosing |
| Gemfibrozil    | 7.6 hours              | 600 mg b.i.d.                                  |

SA AUCs were calculated. Following, relative AUC deviations of SL and SA from the reference values were computed for each DDGI scenario with an exposure marker cost function as shown in Eq. 1:

$$\text{Exposure Marker} = \frac{|AUC_{SL-DDGI} - AUC_{SL-ref}|}{AUC_{SL-ref}} + \frac{|AUC_{SA-DDGI} - AUC_{SA-ref}|}{AUC_{SA-ref}} \quad (1)$$

With Exposure Marker = Relative differences of SL and SA exposure per simvastatin dose as a cost function for dose optimization (the smaller the better),  $AUC_{SL-DDGI}$  = AUC for SL under DDGI condition,  $AUC_{SL-ref}$  = reference AUC for SL,  $AUC_{SA-DDGI}$  = AUC for SA under DDGI condition,  $AUC_{SA-ref}$  = reference AUC for SA.

For each DDGI scenario, the exposure marker cost function was minimized to identify the simvastatin dose with the smallest exposure deviation (matching exposure). For different therapeutic dose levels of simvastatin (20 mg, 40 mg, and 60 mg) relative frequency of recommended doses and the relationship between the number of DDGIs and the optimal dose level were analyzed. Moreover, a hierarchical Euclidian distance cluster analysis stratified against the DDIs and DGIs was performed to identify patterns for generalized dose recommendations. Clustering was computed with complete linkage using the *hclust* function in R.

Results from the dose optimization were transferred into a DDS web application implemented with the R package “shiny,” allowing users to easily filter simulation analysis tailored to DDGIs and simvastatin doses of interest.

## RESULTS

### Simvastatin PBPK model building and evaluation

We successfully developed a whole-body PBPK model of SL and SA. For placebo and DGI model development and evaluation mean data from 57 studies were extracted including 59 SL and 57 SA plasma-concentration time profiles, which represent information from 1,271 study participants. For DGI implementation, plasma-concentration time profiles or AUC and  $C_{max}$  values for *SLCO1B1* (rs4149056) c.521C/C, c.521T/C, c.521T/T, *ABCB1* (rs1128503 rs2032582 and rs1045642) c.1236T-c.2677T-c.3435T, c.1236C-c.2677G-c.3435C, *ABCG2* (rs2231142) c.421A/A, c.421C/A, c.421C/C, and *CYP3A5* (rs776746) *CYP3A5\*3/\*3*, *CYP3A5\*3/\*1*, *CYP3A5\*1/\*1* were used for model development and optimization. System-dependent parameters like reference concentrations and enzyme expression profiles were taken from the PK-Sim database or extracted from literature as described in **Supplementary Material, chapter 1.3**. Doses available for model development and evaluation ranged from 10 mg to 80 mg simvastatin after single and multiple doses.

Extensive model evaluations, as described in the **Supplementary Material, chapter 2.3**, revealed good model performance for placebo PK profiles. Mean ratios predicted vs. observed AUCs were 1 for SL and 0.9 for SA. Mean predicted vs. observed  $C_{max}$  ratios were 0.9 and 0.8 for SL and SA, respectively. GMFE values were 1.3 for SL AUC, 1.5 for SL  $C_{max}$ , 1.5 for SA AUC, and 1.7 for SA  $C_{max}$ , respectively.

### DGI model evaluation

The model was capable to precisely describe and predict the DGI profiles in the training and test datasets. The average AUC ratio was 1.0 for SL and 0.7 for SA, whereas the mean  $C_{max}$  ratio was

0.8 for SL and 0.6 for SA. For DGIs the GMFE values were 1.3 for SL AUC and 1.4 for SL  $C_{max}$ , 1.8 for SA AUC, and 2.2 for SA  $C_{max}$ , respectively (see **Supplementary Material, chapter 2.4.6**). **Figure 2a** shows an example prediction of SA for *SLCO1B1* (rs4149056) c.521C/C and c.521T/T genotype.

### DDI network development

A DDI network was built by coupling models for clarithromycin, gemfibrozil, itraconazole, rifampicin, and midazolam with the newly derived simvastatin model (see **Supplementary Material, chapter 3**). **Figure 2b** shows an example prediction of SL under clarithromycin cotreatment. Mean predicted vs. observed AUC ratios for SL, SA, and midazolam were 1.2, 1.5, and 0.9, respectively. Average predicted vs. observed  $C_{max}$  ratios for SL, SA, and midazolam were 0.9, 1.1, and 1, respectively. GMFE values were 1.3 for both SL AUC and  $C_{max}$ , 1.7 and 1.8 for SA AUC and  $C_{max}$ , as well as 1.1 for both midazolam AUC and  $C_{max}$ .

Moreover, predicted DDI and DGI effect ratios were in good agreement with observed effect ratios, as shown in **Figure 2c**. Overall, only 1 of 18 AUC effect ratios for SL and 1 of 14 AUC effect ratios for SA showed a deviation from the observed effect ratio greater than twofold. **Figure 3** summarizes the metabolic and transportation processes involved in the DDI network and visualizes the relationships between the included compounds and processes.

### Dose optimization

For each simvastatin therapeutic dose (5 to 80 mg in 5 mg steps) 648 DDGIs were optimized, which led to a total of 10,368 DDGI dose recommendations derived from the exposure marker cost function as described in Eq. 1. Cluster analysis revealed that cluster groups differ vastly with several subclusters and no observable pattern (**Figure 4a**). Thus, no generally applicable rule could be established on how to dose simvastatin.

Descriptive statistics revealed that for 13% (60 mg simvastatin therapeutic dose) to 25% (20 mg simvastatin therapeutic dose) of the investigated DDGI scenarios no alternative simvastatin dose could be found. Median optimal dose levels over all investigated DDGIs were 5 mg, 10 mg, and 20 mg for simvastatin therapeutic doses of 20 mg, 40 mg, and 60 mg, respectively. Analyses of the number of DDGIs against the optimal doses revealed a trend for all therapeutic dose levels: a greater number of DDGIs leads toward a lower optimal dose. For a therapeutic dose level of 40 mg, results are visualized in **Figure 4a** (cluster analysis), **Figure 4b** (relative frequency of optimal doses), and **Figure 4c** (number of DDGIs against optimal dose values).

DDGI network simulations were processed and transferred into a web-based interactive decision support system, which can be accessed at [simvastatin.precisiondosing.de](http://simvastatin.precisiondosing.de). The system allows users to investigate simvastatin DDGI situations of interest and explore different scenarios. Here, the user can select a given simvastatin dose, the active comedication, and the *SLCO1B1*, *ABCG2*, and *CYP3A5* genotype. Then, the application presents the optimization results, including recommended dose compared with therapeutic dose and allows the further investigation



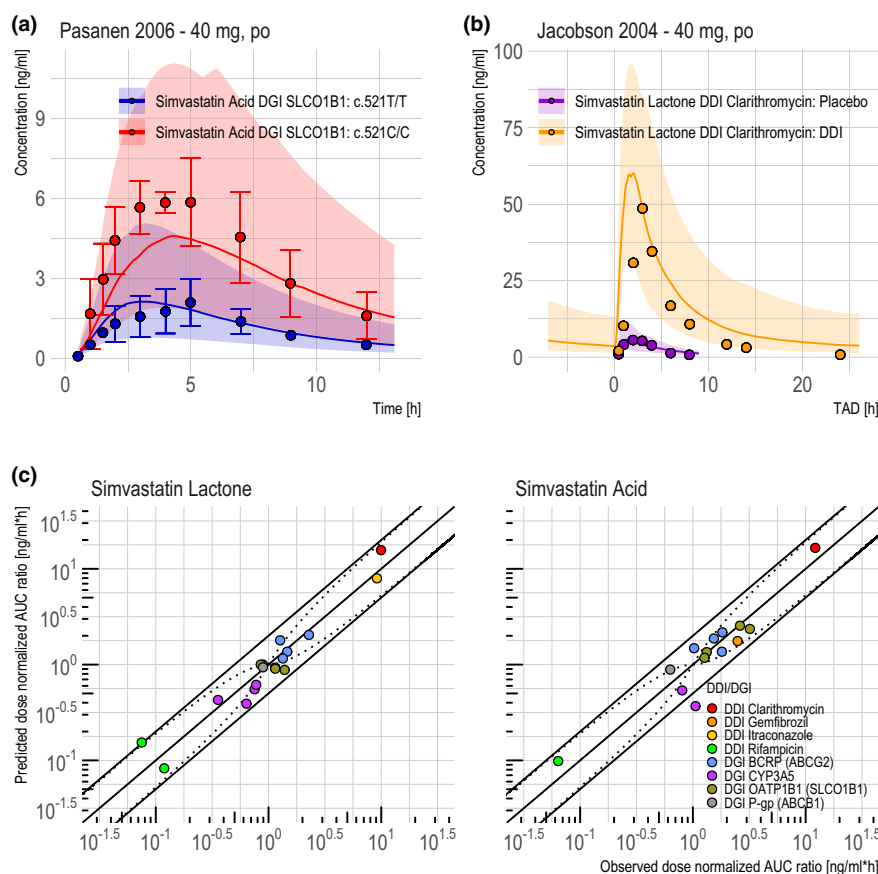


**Figure 2** Example profiles and model evaluation plots for the developed simvastatin PBPK DDGI network. **(a)** Example profiles of the observed vs. predicted simvastatin acid plasma concentration-time profiles for SLC01B1 (rs4149056) c.521C/C, and c.521T/T genotypes.<sup>54</sup> **(b)** Example profiles of the predicted vs. observed simvastatin lactone plasma concentration-time profiles with and without clarithromycin co-treatment.<sup>55</sup> In **a** and **b** dots are observed mean values extracted from literature. Error bars display the observed SDs. Solid lines show the predicted median profile of 100 simulated individuals. Shaded area depicts the predicted 90% confidence interval. **(c)** Depicts the observed vs. predicted dose normalized AUC effect ratios (dose normalized AUC under DDI/DGI conditions divided by dose normalized AUC under placebo conditions). Solid lines show the line of identity as well as the twofold deviations. Dotted lines are the quality limits as proposed by Guest *et al.*<sup>56</sup> AUC, area under the curve; DDGI, drug-drug-gene interaction; DDI, drug-drug interaction; PBPK, physiologicallybased pharmacokinetic. [Colour figure can be viewed at [wileyonlinelibrary.com](http://wileyonlinelibrary.com)]

of SL and SA exposures for the placebo situation, the investigated DDGI situation, and the situation after dose optimization. **Figure 5** depicts case examples analyzed with the support system.

## DISCUSSION

PBPK modeling is increasingly applied during preclinical and clinical development allowing prospective prediction of drug exposure for various scenarios. Investigation of DDIs for regulatory labeling recommendations and problems regarding organ impairment, drug absorption, and pediatric starting dose selection demonstrated the usefulness of this class of mechanistical models in the past.<sup>26</sup> Because DDIs and DGIs can be considered as major drivers of ADRs<sup>2,4,5</sup> the application of PBPK-based MIPD to reduce the incidence of ADRs seems sensible. However, efforts toward the application of physiologically based models for MIPD are still scarce.<sup>12</sup> In this work, we investigated the adaption of PBPK modeling approaches for precision dosing regarding DDGI-sensible compounds in

complex interaction networks and the integration of finding into a decision support system.

Current techniques to address MIPD typically include Bayesian adaptive control methods.<sup>8,27</sup> However, these approaches are limited to interactions, which are already studied and implemented in the model.<sup>8</sup> An extension with other, clinically untested perpetrator or victim drugs or further genetic polymorphisms, is challenging or even impossible. In contrast, PBPK models are well-suited to tackle this limitation and are emphasized by regulatory agencies to investigate new, untested scenarios.<sup>4,8,10–12</sup> At the moment, most whole-body PBPK models purely account for interindividual variability by adapting the physiology of the underlying virtual patient. Hence, the estimation of individual parameters, as it is accomplished in Bayesian methods, is hardly feasible. Consequently, future developments should focus on connecting approaches like maximum *a posteriori* estimation to the realm of PBPK modeling in order to allow PBPK Bayesian techniques to come within reach, combining the best from both worlds. As an application example, such models could use the interindividual variability of a metabolic enzyme

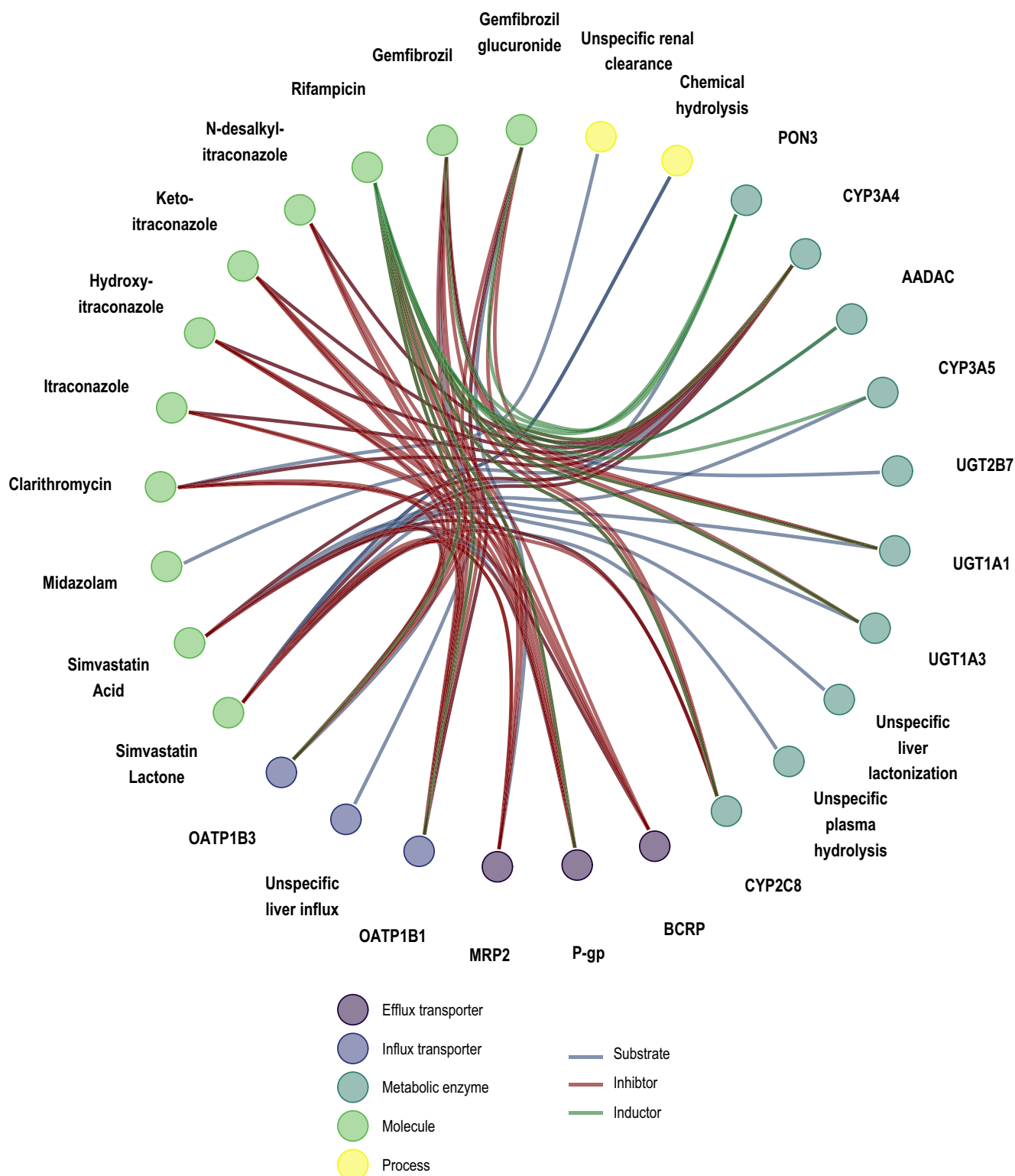


**Figure 3** Relationships between the PK pathways of the compounds included in the presented DDGI network. For the six different drugs simvastatin, itraconazole, rifampicin, gemfibrozil, clarithromycin, and midazolam metabolic, inhibitory and inductive effects are shown as lines. DDGI, drug-drug-gene interaction; PK, pharmacokinetic. [Colour figure can be viewed at [wileyonlinelibrary.com](http://wileyonlinelibrary.com)]

and, based on the measured individual plasma concentration of a harmless reference substance, predict the optimal treatment regime for another compound that is metabolized by this very enzyme. This will require further technical development, the availability of

sufficient individual data, and additional physiological knowledge, but could consequently improve the precision of the PBPK-based MIPD approach. Fortunately, the continuous research efforts, as for example, shown by the open systems pharmacology community,

## Therapeutic dose: 40 mg

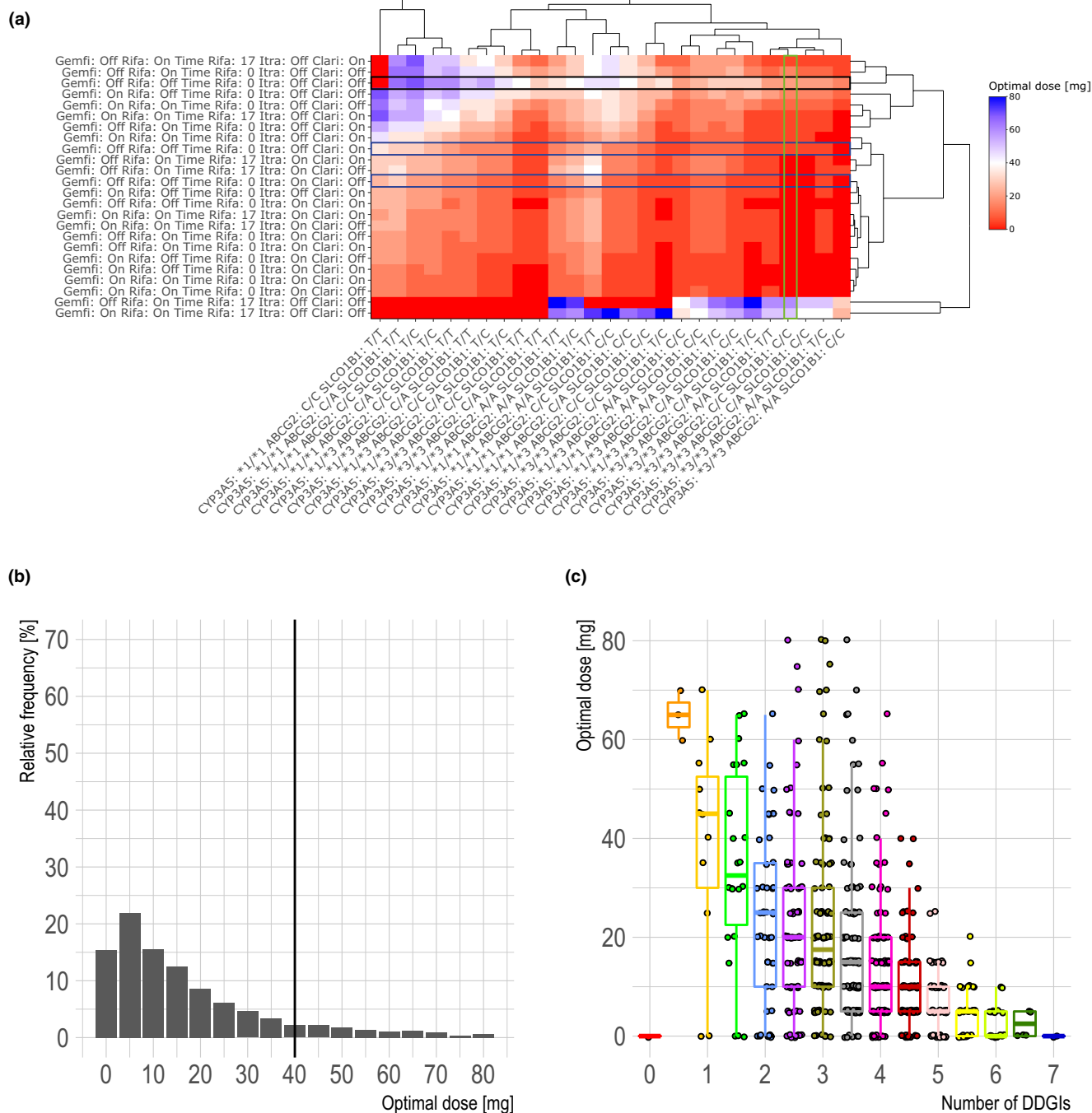


**Figure 4** Results from the dose optimization analysis. (a) Heatmap of the performed cluster analysis. Investigated DDGIs are shown on the x-axis, whereas DDIs are listed on the y-axis. A color-coding as described on the right side of the plot depicts the optimal doses for each DDGI combination. Cluster analysis results are shown as dendrograms on the right and top side of the heatmap. Furthermore, simvastatin treatment without additional DDI-partner, single cotreatment with itraconazole or clarithromycin and the DDGI situation for SLC01B1 (rs4149056) c.521C/C are highlighted with rectangles. (b) Shows the relative distribution of optimal doses for simvastatin. Solid lines depict the therapeutic dose. (c) Boxplots visualizing the number of DDGIs against the optimal simvastatin doses. All boxplots show the following descriptive statistics: The median value, the interquartile range, and the 1.5-fold interquartile range. All analyzes are shown for a therapeutic dose level of 40 mg simvastatin. DDGI, drug-drug-gene interaction; DDI, drug-drug interaction; DGI, drug-gene interaction. [Colour figure can be viewed at [wileyonlinelibrary.com](https://onlinelibrary.com)]

constantly extend the library of available PBPK models and model features.<sup>28</sup> This progressive trend is encouraging that current knowledge and technical gaps can steadily be narrowed.

We demonstrated the applicability of physiologically based precision dosing using the example of simvastatin. Because it is among the drugs most frequently involved in major interactions,

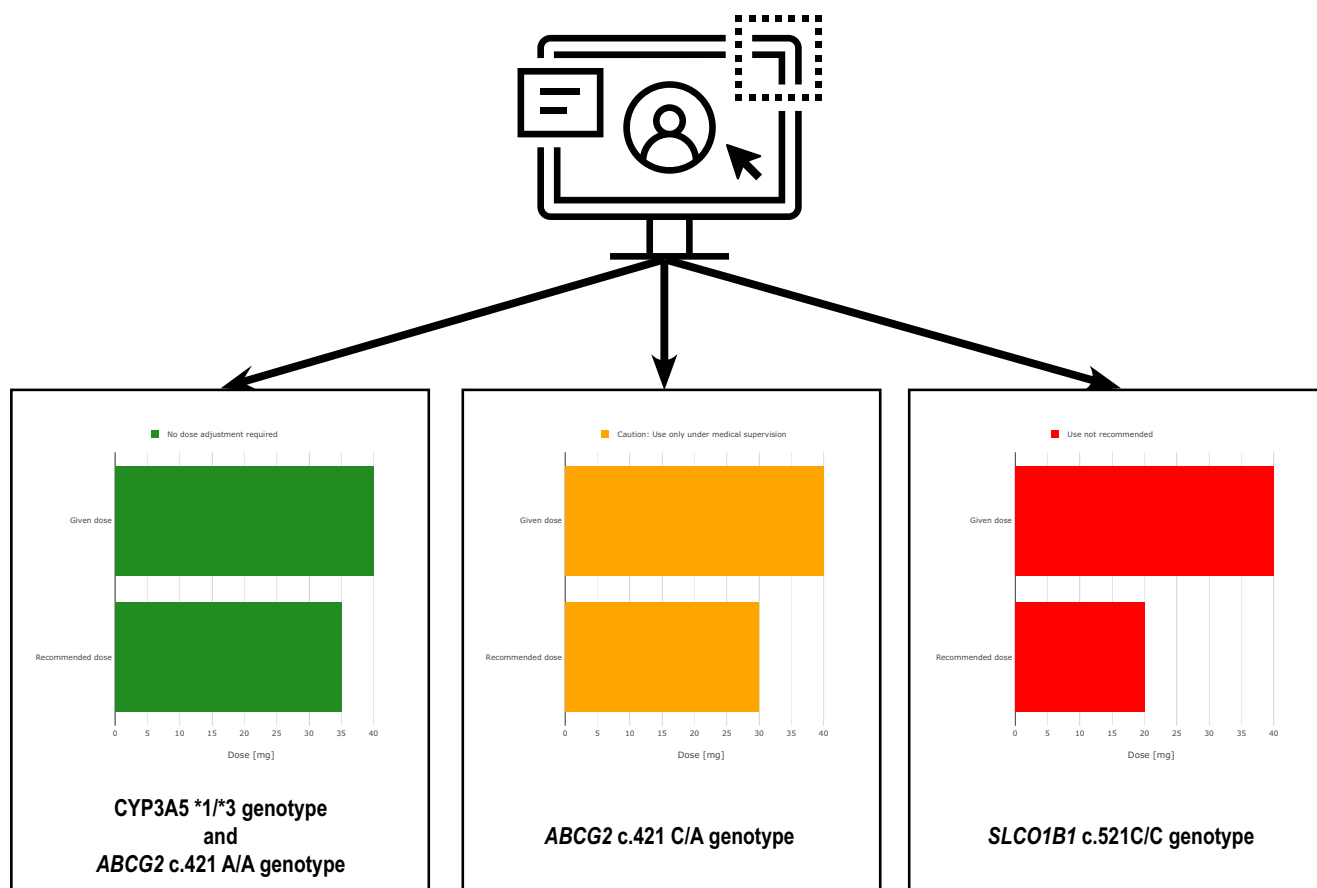


**Figure 5** Case examples analyzed with the developed decision support system. Therapeutic simvastatin dose was 40 mg and SL and SA exposure deviation were equally weighted. From left to right, different recommendations for action are given depending on the deviation between the optimal dose under DDGI condition compared with the therapeutic dose. DDGI, drug-drug-gene interaction; SA, simvastatin acid; SL, simvastatin lactone. [Colour figure can be viewed at [wileyonlinelibrary.com](https://onlinelibrary.wiley.com)]

simvastatin is a perfect candidate to showcase the feasibility of physiologically based dose recommendations for known DGIs and comedication with frequently used DDI partners.<sup>5</sup> For simvastatin, only two whole-body or semimechanistic PBPK models are described in the literature yet.<sup>29,30</sup> Despite good predictive performance for the area of application, they typically focused on a single polymorphism (e.g., *SLCO1B1* (rs4149056)) and one DDI CYP3A4 inhibition effect. In contrast, our work vastly broadens the area of application by the successful development of a newly built whole-body simvastatin PBPK model covering multiple crucial PK processes. Subsequently, the model was connected to a comprehensive DDGI network to extensively study and simulate complex DDGI scenarios. The final model covered four important polymorphisms in the *ABCB1*, *SLCO1B1*, *ABCG2*, and *CYP3A5* genes<sup>20,31–35</sup> relevant for simvastatin's PK and was tested using previously developed and evaluated models for the perpetrators itraconazole, rifampicin, clarithromycin, gemfibrozil, and the victim midazolam.<sup>10–12,23</sup> The simvastatin network showed overall good descriptive and predictive performance and was hence used for further dose optimization analysis. Despite good performance, the model has some limitations, which are primarily caused by insufficient or lacking model input data. For example, for all studies where no information about the genotype was provided,

homozygous wild type genotypes were assumed. Fortunately, the prediction of included placebo profiles with unknown genotype showed that this assumption is sufficient to achieve good model accuracy. Information about the known polymorphism in *ABCB1* was rare and could only be included in the model training dataset and not for testing. Moreover, for some simvastatin PK pathways no data regarding their significance or activity could be gathered (see **Supplementary Material, chapter 2**). Those pathways and associated processes could either not be included in the model or their affinity ( $K_m$ ) or activity ( $k_{cat}$ ) values had to be estimated. Here, additional *in vitro* studies could help to fill this knowledge gaps in the future and, subsequently, further improve the model quality.<sup>36</sup>

Although precision dosing is considered a public health need, the amount and availability of recommendations for adjustments in case of DDGIs, including DDIs and DGIs, are lagging behind. For simvastatin, 5 pharmacogenes are listed on [pharmgkb.org](https://www.pharmgkb.org) as level 2 variants, which equals at least moderate evidence for a significant influence on the pharmacotherapy.<sup>15</sup> Yet, only for one polymorphism in *SLCO1B1* (rs4149056) recommendations on how to adapt the dose are on hand.<sup>15,37,38</sup> For the poor function *SLCO1B1* genotype (c.521C/C) low dosing, prescription of an alternative statin or routine creatine kinase surveillance is typically



recommended.<sup>37,38</sup> Our developed model-based dose recommendations agree on the Clinical Pharmacogenetics Implementation Consortium (CPIC) guideline by also recommending an alternative drug for the *SLCO1B1* c.521C/C polymorphism (see **Figure 5**).<sup>37,38</sup> The FDA drug label of simvastatin (Zocor) contraindicates the concomitant use of strong CYP3A4 inhibitors like itraconazole or clarithromycin.<sup>39</sup> This is also reflected by the presented PBPK DDGI network as shown in **Figure 4a** (red highlighting rectangles) for single clarithromycin or itraconazole cotreatment. Except for DDGIs with some CYP3A5 activity ( $*1/*1$  or  $*1/*3$ ), the model always predicts that no optimal simvastatin dose could be found (optimal dose = 0 mg). This is not surprising, because the originally published clarithromycin and itraconazole models did not include CYP3A5 inhibition (see **Supplementary Material, chapter 3**).<sup>10,23</sup> Although there are hints of CYP3A5 inhibition by itraconazole or clarithromycin in past studies, information available were too sparse to include this process in the models.<sup>40,41</sup> This lack of information is most likely due to the fact that the *CYP3A5*\*3/\*3 nonexpressor genotype is the major genotype in many populations without recent African ancestry. Although only 10–25% of Europeans have detectable levels of hepatic CYP3A5, this rate increases to 55–95% in African Americans.<sup>42–44</sup> For scenarios where CYP3A5 shows activity, it partly replaces the metabolic clearance of CYP3A4 in the network. Whether this holds true and a DDGI with clarithromycin or itraconazole and CYP3A5 only leads to a slightly increased SL exposure should be further investigated.

Apart from individual DDIs or DGIs, there is currently no recommendation for simvastatin DDGIs available.<sup>39</sup> Unfortunately, this is not only the case for simvastatin but reflects the situation for the majority of available drugs.<sup>4</sup> The standard to overcome this deficiency are clinical trials. However, due to the combinatorial explosion of possibilities for complex DDGIs exhaustive investigation via clinical studies is not feasible.<sup>4,9</sup> As shown in the performed cluster analysis (**Figure 4a**) for complicated DDGIs, no generally valid rule or therapy recommendation can be given, making it indeed necessary to investigate DDGIs on an individual level. With the rapid increase in efficiency and availability of computational resources (e.g., via cloud computing) the application of rich PBPK DDGI networks for MIPD, as shown in the presented study, seems feasible. Yet, clinical studies evaluating more complex situations like DDGIs are urgently needed to challenge, refine, and validate MIPD predictions.<sup>12</sup>

Even though the presented work exceeds the number of currently available dose recommendations by far, it still only applies to a small fraction of possible simvastatin DDGIs. Furthermore, it should be noted that dose optimization was only performed for matching exposure and not linked with a pharmacodynamic (PD) model connecting SL and SA exposure with drug efficacy like change in LDL levels or drug toxicity.<sup>43,45,46</sup> Such a PBPK/PD MIPD decision support system could enable clinicians to individually balance therapy risks and chances.<sup>47,48</sup> However, as recent investigations have shown, those models should also regard the exposure of SL, which had not been recognized for a long time.<sup>49</sup> Results from Tahaa *et al.* indicate that SL could be more relevant for drug's toxicity, whereas SA could be more important

for efficacy.<sup>49</sup> For this reason, the exposure marker cost function used for dose optimization was derived from both exposure deviations in order to account for SL exposure deviations as well. By further implementing a weighting factor, the clinician is still free to set the influence for both species individually. Nevertheless, this highlights that further models and model extensions are required to enlarge the current network. Fortunately, the established PBPK network shows enough flexibility to be extended as soon as more models for PD effects, perpetrator, or victim compounds are available.<sup>10–12,23</sup> Such models can then easily be linked with the current network and subsequently be used for further optimizations.<sup>10–12,23</sup>

The simulation analyses for DDGI scenarios were simulated for 7 days + 24 hours postdose. Although, for single drug treatment, this simulation time should be sufficient to reach PK steady-state conditions for all compounds investigated,<sup>50–53</sup> this assumption might not hold true for complex DDGI scenarios. However, as *a priori* effect estimations of complex DDGI scenarios on drug half-lives is not feasible, this should be considered for any follow-up simulation analysis.

As stated by Gonzalez and coworkers, a precision dosing strategy for clinical practice does not only rely on the development of predictive dosing models, but also on the integration into a decision support system accessible by the physician.<sup>8</sup> Thus, we provide an exemplary implementation of such a system for simvastatin to demonstrate ease of use for modeling nonexperts via a web-based solution.

In conclusion, a novel physiologically based precision dosing approach was successfully developed to study complex DDGI network scenarios for the model drug simvastatin. Findings from extensive cluster analysis of various DDGIs showed no generalized pattern for dose adjustments suggesting the need for individualized MIPD approaches to ensure effectiveness of therapy and prevention of severe ADRs. It could be demonstrated that adaption of whole-body PBPK modeling for MIPD allows the flexible extension and requalification of already established interaction networks more easily and with greater confidence for unknown scenarios than already established tooling for MIPD. Future developments should focus on enhancing the capabilities of PBPK modeling by integration of Bayesian adaptive control mechanisms like maximum *a posteriori* estimation allowing more fine-grained personalized readjustment for DDI-sensible and DGI-sensible drugs. Efforts for open access model deployment should be promoted for more widespread utilization. Besides open access to models, the integration with easy to use decision support systems is crucial to allow the adaption into clinical practice. Thus, for further use, all simvastatin DDGI network model files are publicly available (<https://github.com/Clinical-Pharmacy-Saarland-University>) and the physiologically based precision dosing decision support system is deployed for open access at [simvastatin.precisiondosing.de](http://simvastatin.precisiondosing.de).

#### SUPPORTING INFORMATION

Supplementary information accompanies this paper on the *Clinical Pharmacology & Therapeutics* website ([www.cpt-journal.com](http://www.cpt-journal.com)).

#### FUNDING

This work was funded by the Robert Bosch Stiftung (Stuttgart, Germany), the European Commission Horizon 2020 UPGx grant 668353, a grant

from the German Federal Ministry of Education and Research (BMBF 031L0188D), and the Deutsche Forschungsgemeinschaft (DFG, German Research Foundation) under Germany's Excellence Strategy—EXC 2180—390900677.

#### ACKNOWLEDGMENTS

Open access funding enabled and organized by Projekt DEAL.

#### CONFLICT OF INTEREST

The authors declared no competing interests for this work.

#### AUTHOR CONTRIBUTIONS

J.-G.W., D.S., M.S., and T.L. wrote the manuscript. J.-G.W., M.S., and T.L. designed the research. J.-G.W. performed the research. J.-G.W., D.S., and T.L. analyzed the data.

© 2020 The Authors. *Clinical Pharmacology & Therapeutics* published by Wiley Periodicals LLC on behalf of American Society for Clinical Pharmacology and Therapeutics.

This is an open access article under the terms of the Creative Commons Attribution-NonCommercial License, which permits use, distribution and reproduction in any medium, provided the original work is properly cited and is not used for commercial purposes.

- Elsevier. Elsevier joins forces with pharmaceutical industry leaders to build new drug-drug interaction risk calculator <<https://www.elsevier.com/about/press-releases/clinical-solutions/elsevier-joins-forces-with-pharmaceutical-industry-leaders-to-build-new-drug-drug-interaction-risk-calculator>> (2019). Accessed July 12, 2020.
- US Food and Drug Administration. Preventable adverse drug reactions: a focus on drug interactions <<https://www.fda.gov/drugs/drug-interactions-labeling/preventable-adverse-drug-reactions-focus-drug-interactions>> (2018). Accessed July 12, 2020.
- Carr, T. Too many meds? America's love affair with prescription medication <<https://www.consumerreports.org/prescription-on-drugs/too-many-meds-americas-love-affair-with-prescription-medication/>> (2017). Accessed July 12, 2020.
- Malki, M.A. & Pearson, E.R. Drug-drug-gene interactions and adverse drug reactions. *Pharmacogenomics J.* **20**, 355–366 (2020).
- Verbeurgt, P., Mamiya, T. & Oesterheld, J. How common are drug and gene interactions? Prevalence in a sample of 1143 patients with CYP2C9, CYP2C19 and CYP2D6 genotyping. *Pharmacogenomics* **15**, 655–665 (2014).
- Routledge, P.A., O'Mahony, M.S. & Woodhouse, K.W. Adverse drug reactions in elderly patients. *Br. J. Clin. Pharmacol.* **57**, 121–126 (2004).
- Alhawassi, T.M., Krass, I., Bajorek, B.V. & Pont, L.G. A systematic review of the prevalence and risk factors for adverse drug reactions in the elderly in the acute care setting. *Clin. Interv. Aging* **9**, 2079–2086 (2014).
- Gonzalez, D. et al. Precision dosing: public health need, proposed framework, and anticipated impact. *Clin. Transl. Sci.* **10**, 443–454 (2017).
- Tornio, A., Filppula, A.M., Niemi, M. & Backman, J.T. Clinical studies on drug-drug interactions involving metabolism and transport: methodology, pitfalls, and interpretation. *Clin. Pharmacol. Ther.* **105**, 1345–1361 (2019).
- Britz, H. et al. Physiologically-based pharmacokinetic models for CYP1A2 drug-drug interaction prediction: a modeling network of fluvoxamine, theophylline, caffeine, rifampicin, and midazolam. *CPT Pharmacometrics Syst. Pharmacol.* **8**, 296–307 (2019).
- Hanke, N. et al. PBPK models for CYP3A4 and P-gp DDI prediction: a modeling network of rifampicin, itraconazole, clarithromycin, midazolam, alfentanil, and digoxin. *CPT Pharmacometrics Syst. Pharmacol.* **7**, 647–659 (2018).
- Türk, D. et al. Physiologically based pharmacokinetic models for prediction of complex CYP2C8 and OATP1B1 (SLCO1B1) drug–drug–gene interactions: a modeling network of gemfibrozil, repaglinide, pioglitazone, rifampicin, clarithromycin and itraconazole. *Clin. Pharmacokinet.* **58**, 1595–1607 (2019).
- Mendes, P., Robles, P.G. & Mathur, S. Statin-induced rhabdomyolysis: a comprehensive review of case reports. *Physiother. Can.* **66**, 124–132 (2014).
- Drugs.com. Simvastatin drug interactions <<https://www.drugs.com/drug-interactions/simvastatin.html>> Accessed July 5, 2020.
- Whirl-Carrillo, M. et al. Pharmacogenomics knowledge for personalized medicine. *Clin. Pharmacol. Ther.* **92**, 414–417 (2012).
- Talreja, O., Kerndt, C.C. & Cassagnol, M.S. StatPearls <<http://www.ncbi.nlm.nih.gov/pubmed/30422514>> (2020). Accessed July 31, 2020.
- Moßhammer, D., Schaeffeler, E., Schwab, M. & Mörike, K. Mechanisms and assessment of statin-related muscular adverse effects. *Br. J. Clin. Pharmacol.* **78**, 454–466 (2014).
- IQVIA Institute for Human Data Science. Medicine use and spending in the U.S. <<https://www.iqvia.com/insights/the-iqvia-institute/reports/medicine-use-and-spending-in-the-us-a-review-of-2018-and-outlook-to-2023>> (2019).
- Open Systems Pharmacology Community. Open systems pharmacology suite <[www.open-systems-pharmacology.org](http://www.open-systems-pharmacology.org)> (2019). Accessed July 31, 2020.
- Wojtyniak, J., Britz, H., Selzer, D., Schwab, M. & Lehr, T. Data digitizing: accurate and precise data extraction for quantitative systems pharmacology and physiologically-based pharmacokinetic modeling. *CPT Pharmacometrics Syst. Pharmacol.* **9**, 322–331 (2020).
- R Core Team. *R: A Language and Environment for Statistical Computing* <<https://www.r-project.org>> (2020).
- Hanke, N. et al. PBPK models for CYP3A4 and P-gp DDI prediction: a modeling network of rifampicin, itraconazole, clarithromycin, midazolam, alfentanil, and digoxin. *CPT Pharmacometrics Syst. Pharmacol.* **7**, 647–659 (2018).
- Moj, D. et al. Clarithromycin, midazolam, and digoxin: application of PBPK modeling to gain new insights into drug-drug interactions and co-medication regimens. *AAPS J.* **19**, 298–312 (2017).
- Edginton, A.N., Schmitt, W. & Willmann, S. Development and evaluation of a generic physiologically based pharmacokinetic model for children. *Clin. Pharmacokinet.* **45**, 1013–1034 (2006).
- Morley, S.K., Brito, T.V. & Welling, D.T. Measures of model performance based on the log accuracy ratio. *Space Weather* **16**, 69–88 (2018).
- Wagner, C. et al. Application of physiologically based pharmacokinetic (PBPK) modeling to support dose selection: report of an FDA public workshop on PBPK. *CPT Pharmacometrics Syst. Pharmacol.* **4**, 226–230 (2015).
- Mould, D.R., D'Haens, G. & Upton, R.N. Clinical decision support tools: the evolution of a revolution. *Clin. Pharmacol. Ther.* **99**, 405–418 (2016).
- Lippert, J. et al. Open systems pharmacology community—an open access, open source, open science approach to modeling and simulation in pharmaceutical sciences. *CPT Pharmacometrics Syst. Pharmacol.* **8**, 878–882 (2019).
- Lippert, J. et al. A mechanistic, model-based approach to safety assessment in clinical development. *CPT Pharmacometrics Syst. Pharmacol.* **1**, e13 (2012).
- Tsamandouras, N. et al. Development and application of a mechanistic pharmacokinetic model for simvastatin and its active metabolite simvastatin acid using an integrated population PBPK approach. *Pharm. Res.* **32**, 1864–1883 (2015).
- Kim, K.-A., Park, P.-W., Lee, O.-J., Kang, D.-K. & Park, J.-Y. Effect of polymorphic CYP3A5 genotype on the single-dose simvastatin pharmacokinetics in healthy subjects. *J. Clin. Pharmacol.* **47**, 87–93 (2007).

32. Choi, H.Y. *et al.* Impact of CYP2D6, CYP3A5, CYP2C19, CYP2A6, SLC01B1, ABCB1, and ABCG2 gene polymorphisms on the pharmacokinetics of simvastatin and simvastatin acid. *Pharmacogenet. Genomics* **25**, 595–608 (2015).
33. Pasanen, M.K., Neuvonen, M., Neuvonen, P.J. & Niemi, M. SLC01B1 polymorphism markedly affects the pharmacokinetics of simvastatin acid. *Pharmacogenet. Genomics* **16**, 873–879 (2006).
34. Keskitalo, J.E., Pasanen, M.K., Neuvonen, P.J. & Niemi, M. Different effects of the ABCG2 c.421C>A SNP on the pharmacokinetics of fluvastatin, pravastatin and simvastatin. *Pharmacogenomics* **10**, 1617–1624 (2009).
35. Keskitalo, J.E., Kurkinen, K.J., Neuvonen, P.J. & Niemi, M. ABCB1 haplotypes differentially affect the pharmacokinetics of the acid and lactone forms of simvastatin and atorvastatin. *Clin. Pharmacol. Ther.* **84**, 457–461 (2008).
36. Kuepfer, L. *et al.* Applied concepts in PBPK modeling: how to build a PBPK/PD model. *CPT Pharmacometrics Syst. Pharmacol.* **5**, 516–531 (2016).
37. Bank, P. *et al.* Comparison of the Guidelines of the Clinical Pharmacogenetics Implementation Consortium and the Dutch Pharmacogenetics Working Group. *Clin. Pharmacol. Ther.* **103**, 599–618 (2018).
38. Ramsey, L.B. *et al.* The clinical pharmacogenetics implementation consortium guideline for SLC01B1 and simvastatin-induced myopathy: 2014 update. *Clin. Pharmacol. Ther.* **96**, 423–428 (2014).
39. Merck & Co., Inc. Zocor (Simvastatin) [package insert]. U.S. Food and Drug Administration website <[https://www.accessdata.fda.gov/drugsatfda\\_docs/label/2019/019766s100lbl.pdf](https://www.accessdata.fda.gov/drugsatfda_docs/label/2019/019766s100lbl.pdf)> Accessed July 5, 2020.
40. Shirasaka, Y. *et al.* Effect of CYP3A5 expression on the inhibition of CYP3A-catalyzed drug metabolism: impact on modeling CYP3A-mediated drug-drug interactions. *Drug Metab. Dispos.* **41**, 1566–1574 (2013).
41. Michaud, V. & Turgeon, J. Assessment of competitive and mechanism-based inhibition by clarithromycin: use of domperidone as a CYP3A probe-drug substrate and various enzymatic sources including a new cell-based assay with freshly isolated human hepatocytes. *Drug Metab. Lett.* **4**, 69–76 (2010).
42. Bains, R.K. *et al.* Molecular diversity and population structure at the cytochrome P450 3A5 gene in Africa. *BMC Genet.* **14**, 34 (2013).
43. Scherer, N., Dings, C., Böhm, M., Laufs, U. & Lehr, T. Alternative treatment regimens with the PCSK9 inhibitors alirocumab and evolocumab: a pharmacokinetic and pharmacodynamic modeling approach. *J. Clin. Pharmacol.* **57**, 846–854 (2017).
44. Kuehl, P. *et al.* Sequence diversity in CYP3A promoters and characterization of the genetic basis of polymorphic CYP3A5 expression. *Nat. Genet.* **27**, 383–391 (2001).
45. Kim, J. *et al.* A population pharmacokinetic-pharmacodynamic model for simvastatin that predicts low-density lipoprotein-cholesterol reduction in patients with primary hyperlipidaemia. *Basic Clin. Pharmacol. Toxicol.* **109**, 156–163 (2011).
46. Tsamandouras, N. *et al.* Identification of the effect of multiple polymorphisms on the pharmacokinetics of simvastatin and simvastatin acid using a population-modeling approach. *Clin. Pharmacol. Ther.* **96**, 90–100 (2014).
47. Marshall, S. *et al.* Model-informed drug discovery and development: current industry good practice and regulatory expectations and future perspectives. *CPT Pharmacometrics Syst. Pharmacol.* **8**, 87–96 (2019).
48. EFPIA MID3 Workgroup, *et al.* Good practices in model-informed drug discovery and development: practice, application, and documentation. *CPT Pharmacometrics Syst. Pharmacol.* **5**, 93–122 (2016).
49. Taha, D.A. *et al.* The role of acid-base imbalance in statin-induced myotoxicity. *Transl. Res.* **174**, 140–160.e14 (2016).
50. Todd, P.A. & Ward, A.G. A review of its pharmacodynamic and pharmacokinetic properties, and therapeutic use in dyslipidaemia. *Drugs* **36**, 314–339 (1988).
51. Acocella, G. Clinical pharmacokinetics of rifampicin. *Clin. Pharmacokinet.* **3**, 108–127 (1978).
52. Heykants, J. *et al.* The clinical pharmacokinetics of itraconazole: an overview. *Mycoses* **32**(suppl. 1), 67–87 (1989).
53. Rodvold, K.A. Clinical pharmacokinetics of clarithromycin. *Clin. Pharmacokinet.* **37**, 385–398 (1999).
54. Pasanen, M.K., Fredrikson, H., Neuvonen, P.J. & Niemi, M. Different effects of SLC01B1 polymorphism on the pharmacokinetics of atorvastatin and rosuvastatin. *Clin. Pharmacol. Ther.* **82**, 726–733 (2007).
55. Jacobson, T.A. Comparative pharmacokinetic interaction profiles of pravastatin, simvastatin, and atorvastatin when coadministered with cytochrome P450 inhibitors. *Am. J. Cardiol.* **94**, 1140–1146 (2004).
56. Guest, E.J., Aarons, L., Houston, J.B., Rostami-Hodjegan, A. & Galetin, A. Critique of the two-fold measure of prediction success for ratios: application for the assessment of drug-drug interactions. *Drug Metab. Dispos.* **39**, 170–173 (2011).